

Multifractality of the Lorenz system

Kjell Ottar Wiklund and John N. Elgin

Department of Mathematics, Imperial College, 180 Queen's Gate, London SW7 2BZ, United Kingdom

(Received 12 March 1996)

We use the unstable periodic orbit expansion of the dynamical ζ function to find the multifractal spectra $f(\alpha)$ and $g(\Lambda)$ for the Lorenz system at $(r, \sigma, b) = (28, 10, 8/3)$ and also for an incomplete, generalized Baker's map with the topology of the Lorenz system. [S1063-651X(96)01908-3]

PACS number(s): 05.45.+b, 02.50.Cw, 02.60.Cb

I. INTRODUCTION

The multifractal properties of a chaotic attractor are usefully quantified by its spectrum of singularities $f(\alpha)$ [1]. Here $\alpha \in [\alpha_{\min}, \alpha_{\max}]$ is the pointwise dimension, or Hölder exponent, of the natural measure μ at point x_i on the attractor and is defined by the relation

$$\alpha(x_i) = \lim_{l_i \rightarrow 0} \frac{\ln \mu[S(l_i, x_i)]}{\ln l_i}, \quad (1)$$

where $S(l_i, x_i)$ denotes a segment in an optimal partition to be specified below and l_i is the diameter of the smallest ball containing S . As the partition becomes infinitely refined, S shrinks onto the point x_i . $f(\alpha)$ is then the Hausdorff dimension of the collection of all points with pointwise dimension α .

Within a more general thermodynamical formalism, the singularity spectrum is one of several ways in which the attractor properties can be quantified and contains the information in the generalized dimensions D_q [2]. A different measure of complexity is the spectrum of dynamical scaling indices $g(\Lambda)$, where Λ_i is the local Liapunov exponent at point x_i and $g(\Lambda_i)$ is the topological entropy of the collection of points with exponent Λ_i [3]. This spectrum contains the information in the set of Rényi (generalized) entropies [4].

Recent implementations of this descriptive approach have made imaginative use of the dynamical ζ function and, in particular, the way this function can be expressed through the cycle expansions [5]. Here

$$\frac{1}{\zeta} = \prod_{\text{PC}} (1 - t_p), \quad (2)$$

where the product is over a set of representative periodic orbits, the prime cycles (PC). The prime cycles are found from the set of periodic orbits by removing the orbits that are repetitions of lower-order orbits. The weight t_p attached to each prime cycle is determined by the quantities of interest, as discussed in detail in [5], and in Sec. II B below. The leading zero of $1/\zeta$ is then sought, which in turn determines the required spectrum.

The strength of this approach is that the infinite product (2) is often closely approximated by a finite expansion over a set of low-order prime cycles—the fundamental cycles—

thereby reducing the computational problem of finding the leading zero. This has far-reaching consequences for the description of chaotic systems: Even though trajectories themselves cannot be followed for long times, a class of quantities can be found in an averaged sense. Specifically, we can find the multifractal spectra $f(\alpha)$ and $g(\Lambda)$. Numerically calculated trajectories are, via the shadowing theorem of Bowen and Anosov, close to a "true" trajectory of the system, but are of little use in a multifractal description, as we then must describe *any* behavior the system might show, not just the measure-one behavior.

The purpose of this article is to demonstrate the application of this technique to a system of ordinary differential equations. The results of similar studies for maps have appeared in the literature, but to date application of the technique to flows has been restricted to determining the Hausdorff dimension and the Liapunov exponent [6,7]. Here we compute the complete spectra using a formalism that shows where in the spectra a given cycle contributes. Two aspects will be investigated in detail.

(i) Although it will prove possible to encode each periodic orbit with a binary label, the binary dynamics in our system is incomplete, implying that not every string corresponds to an allowed periodic orbit. This is denoted a "pruned" binary dynamics, since not all branches of the complete binary tree are covered. By utilizing the binary grammar, the symbolic dynamics can be renormalized to a complete dynamics of higher order. We can then find a special family of orbits giving the main part of $1/\zeta$, while other orbits contribute only through higher-order terms.

(ii) In a more general case, we will not be able to renormalize the symbolic dynamics, i.e., the symbolic dynamics will not be a finite shift. We will discuss how this affects the expansion of $1/\zeta$.

In Sec. III we explore the Lorenz system [8]

$$\begin{aligned} \dot{x} &= \sigma(y - x), \\ \dot{y} &= x(r - z) - y, \\ \dot{z} &= xy - bz \end{aligned} \quad (3)$$

at parameter values $(\sigma, b, r) = (10, 8/3, \sim 28)$, i.e., r varies over a small range near 28. To illustrate the technique and to facilitate discussion of results presented in Sec. III, we look first in Sec. II at a pruned generalized Baker's map.

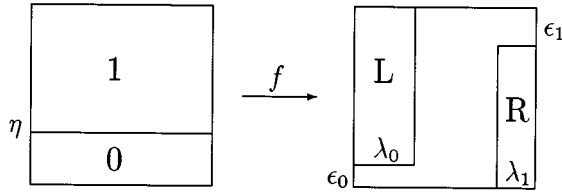


FIG. 1. First coarse graining of the pruned, generalized Baker's map f of Eq. (4). The part marked 0 is mapped onto L , whereas the region 1 is mapped onto R .

II. A PRUNED, GENERALIZED BAKER'S MAP

Consider the map f of the unit square given by

$$\begin{pmatrix} x_{n+1} \\ y_{n+1} \end{pmatrix} = \begin{cases} \begin{pmatrix} \lambda_0 x_n \\ \epsilon_0 + \Lambda_0 y_n \end{pmatrix}, & y_n \in [0, \eta] \\ \begin{pmatrix} 1 - \lambda_1 (1 - x_n) \\ (y_n - \eta) \Lambda_1 \end{pmatrix}, & y_n \in (\eta, 1]. \end{cases} \quad (4)$$

Referring to Fig. 1, $\Lambda_0 = (1 - \epsilon_0)/\eta$ and $\Lambda_1 = (1 - \epsilon_1)/(1 - \eta)$ are the expansion factors in regions 0 and 1 and $\lambda_0, \lambda_1, \eta, \epsilon_0$, and ϵ_1 are all in $(0, 1)$. The periodic orbits of this map are first encoded with a binary label: here a 0 each time an iterate lands in $y < \eta$, otherwise a 1. Each periodic orbit is then uniquely represented by its appropriate binary string. Next we prune, by requiring that no periodic orbit has more than i_0 successive visits to region 0, nor more than i_1 successive visits to region 1. This restriction, called a block pruning rule, can be effected through a particular choice of the parameters ϵ_0 and ϵ_1 . When ϵ_0 and ϵ_1 are small, $i_0 \sim -\ln \epsilon_0 / \ln 2$ and $i_1 \sim -\ln \epsilon_1 / \ln 2$. The complete binary dynamics is regained when ϵ_0 and ϵ_1 are set to 0.

A. Cycle expansions of the pruned Baker's map

Calculating the product of (2) the direct way, we get the expansion

$$\frac{1}{\zeta} = 1 - \sum_{p \in \text{PPC}} t_p,$$

where PPC is the power set of PC, i.e., the set of all different combinations of prime cycles. To facilitate the computation of $1/\zeta$, it is useful to write it in the cycle expanded form of [5]

$$\frac{1}{\zeta} = 1 - \sum_{f \in \text{FC}} t_f - \sum_{n > 0} c_n, \quad (5)$$

where FC denotes the fundamental cycles and c_n is the remaining contribution from elements of PPC of length n , also called the n th level curvature correction. The multinomial structure of the pruned Baker's map (4) ensures that $c_n = 0$ for all n , since the weight t_p depends only on the number of zeros and ones in the binary label of the orbit p . For the

Lorenz system, however, the multinomial structure is only approximate and the low-order corrections must be taken into consideration.

The pruning rule implies that whenever the itinerary of a periodic orbit changes from 1 to 0, not more than i_0 zeros follow, and if the symbol changes from 0 to 1, not more than i_1 ones follow. We can use this to introduce a more efficient symbolic dynamics, where the new symbols are the $i_0 \times i_1$ binary strings of the form $0^k 1^l$, for $k \in [1, i_0]$ and $l \in [1, i_1]$. Creating all combinations of these new symbols, we can label all periodic orbits, without any unused strings, showing that the binary dynamics pruned in this special way is complete multinary, of order $i_0 \times i_1$.

The multinomial structure of the pruned Baker's map gives a weight of the form $t_p = a^{n_0} b^{n_1}$, where n_0 and n_1 denote the number of zeros and ones in the binary label of the periodic orbit p , of symbolic length $n_p = n_0 + n_1$. The fundamental cycles will then be the new symbols: $\text{FC} = \{0^k 1^l\}$ with k and l as above. The expansion (5) is thus readily evaluated to give

$$\frac{1}{\zeta} = 1 - \frac{ab(1-a^{i_0})(1-b^{i_1})}{(1-a)(1-b)}. \quad (6)$$

Introducing the "dressed" variables $A = a(1-a^{i_0})/(1-a^{i_0+1})$ and $B = b(1-b^{i_1})/(1-b^{i_1+1})$, this can be written $1/\zeta = 1 - AB/[(1-A)(1-B)]$. Setting $1/\zeta = 0$ then yields $A + B = 1$. For complete binary dynamics, i_0 and $i_1 \rightarrow \infty$, $A = a$, and $B = b$. The choice for a and b now depends on the particular thermodynamic aspect we wish to examine. Some examples follow.

B. Multifractality of the pruned Baker's map

We now examine some thermodynamic properties of the map, beginning with the spectrum of singularities $f(\alpha)$. In principle [1], this is computed from the partition function

$$\Gamma(q, \tau) = \lim_{n \rightarrow \infty} \sum_{\sigma_n(q)} p_i^q l_i^{-\tau}, \quad (7)$$

where $\sigma_n(q)$ is an optimal partition from \mathcal{Z}_n , the set of all partitions with n segments, the optimization given by a supremum when $q > 1$, and an infimum when $q \leq 1$. The size l_i of a segment is the diameter of the smallest ball containing the segment, whereas the measure contained in the segment is p_i . For a given $q \in \mathbb{R}$, $\tau(q)$ is found as the unique τ , where $\Gamma(q, \tau)$ flips from 0 to ∞ . The pointwise dimension is then found from the definition $\alpha = d\tau/dq$ and a Legendre transform determines the spectrum of singularities: $f(\alpha) = q\alpha - \tau(q)$.

There are two practical difficulties with the partition function in (7): first of all, the optimal partition has to be found and second, we need appropriate quantities representing the distribution of visitation frequencies $\{p_i\}$ and the lengths $\{l_i\}$. For the first problem it is usually argued [9] that one can use the Kolmogorov-Sinai theorem of ergodic theory and that the Shannon entropy $\sum_{\sigma} p_i \ln p_i$ thus takes its supremum value when the partition σ is generating. However, this theorem is not automatically applicable to a partition function of

the form (7), since the proof [10] uses the properties of the Shannon entropy, quite different from the properties of (7).

A generalization of the Kolmogorov-Sinai theorem can be found [11] in the case of the Rényi entropy, showing that

$$\sup_{\xi \in \mathcal{Z}_n} \left(\frac{\ln \sum \xi p_i^q}{1-q} \right) = \frac{\ln \sum \gamma p_i^q}{1-q} \quad (8)$$

when γ is a generating partition for the system. For expansive homeomorphisms, a uniform partition is generating when the mesh is finer than the expansive constant [12]. The sum in (7) can then be written $l_n^{-\tau} \sum \sigma p_i^q$, where σ is the optimal partition. The split optimum defining σ in (7) can be formulated as a supremum, since

$$\frac{\ln \sum \sigma p_i^q}{1-q} = \sup_{\xi \in \mathcal{Z}_n} \left(\frac{\ln \sum \xi p_i^q}{1-q} \right),$$

and (8) applies, showing that a generating partition is optimal also for (7).

For the Baker's map, and for a suitable Poincaré map of the Lorenz equations, we can find a generating partition consistent with a binary symbolic dynamics. To each point there is then a unique semi-infinite binary string, or itinerary, generated by the trajectory from that point. On the n th level of coarse graining each segment is a collection of the points with identical n itinerary and this can be used to label each segment uniquely.

Each segment contains a periodic orbit whose symbolic representation is just infinite repetitions of the binary label of the segment, and the visitation frequency and size of the segment can be represented by the properties of this periodic orbit. In this way Grebogi, Ott, and Yorke [13] argue that for Markov partitions, (7) can be written

$$\Gamma(q, \tau) = \lim_{n \rightarrow \infty} \sum_{j \in \mathcal{F}_n} \Lambda_j^{-q} \lambda_j^{q-\tau-1}, \quad (9)$$

where \mathcal{F}_n is the set of all fixed points of f^n , whereas Λ_j and λ_j are the absolute values of the unstable and stable eigenvalues (Floquet multipliers) of the fixed point j . The partition defined above is Markovian since, by construction, the boundaries of the $(n+1)$ th partition maps to the boundaries of the n th partition.

Though simplified, it is still a difficult and suboptimal task to calculate this sum accurately. We will see that use of the ζ function incorporates the fact that the properties of periodic orbits are given in finite time, but persist forever, enabling an efficient resummation.

To get from Eq. (9) to the ζ function in Eq. (2), first introduce the level- n partition sum $\Gamma_n(q, \tau)$, so that $\Gamma = \Gamma_{n \rightarrow \infty}$. Then introduce the generating function $\Omega(z; q, \tau) = \sum_{n > 0} z^n \Gamma_n(q, \tau)$. After judicious rearrangement of the terms [5], Ω can be expressed in the form

$$\Omega(z; q, \tau) = -z \frac{d}{dz} \ln \prod_{p \in \text{PC}} [1 - z^{n_p} t_p(q, \tau)],$$

where n_p is the length of the prime cycle p and $t_p = \Lambda_p^{-q} \lambda_p^{q-\tau-1}$. With $z=1$, the requirement $\Gamma(q, \tau) = 1$ corresponds to finding the leading zero of $1/\zeta$.

Consider the pruned baker's map of Eq. (4): Any periodic orbit p of length n_p , containing n_0 zeros and n_1 ones, has the multipliers $\Lambda_p = \Lambda_0^{n_0} \Lambda_1^{n_1}$ and $\lambda_p = \lambda_0^{n_0} \lambda_1^{n_1}$, where $\Lambda_0, \Lambda_1, \lambda_0$ and λ_1 are as in (4). With the orbit p , we now associate the weight $t_p = \Lambda_p^{-q} \lambda_p^{q-\tau-1}$, which on using the above equations becomes $t_p = a^{n_0} b^{n_1}$, if $a = \Lambda_0^{-q} \lambda_0^{q-\tau-1}$ and $b = \Lambda_1^{-q} \lambda_1^{q-\tau-1}$.

Having identified a and b , Eq. (6) applies and the leading zero of $1/\zeta$ determines the required $\tau(q)$. A comparison between this formalism and the finite partition sum (9) shows that we now include all orbits found and that each orbit is infinitely recycled; i.e., an infinite resummation of each periodic orbit is done.

It is instructive to evaluate $\alpha(q)$ formally through a variation of Eq. (5) with respect to q and τ : $dq \partial_q \zeta^{-1} + d\tau \partial_\tau \zeta^{-1} = 0$, and then use $\alpha(q) = d\tau/dq$ to find

$$\alpha(q) = 1 - \frac{\langle \ln \Lambda \rangle}{\langle \ln \lambda \rangle}. \quad (10)$$

Here and throughout this article, the angular brackets are used to denote an ensemble average, which we will call the escort average, which in this case takes the form

$$\langle Q \rangle \equiv \sum_{f \in \text{FC}} t_f Q_f, \quad (11)$$

with weights $t_f = \Lambda_f^{-q} \lambda_f^{q-\tau(q)-1}$. In general, this average will have to be taken over the power set of the prime cycles PPC.

In the $f(\alpha)$ formalism $\alpha(1) = D_1$, the information dimension. When $q=1$, the escort average is an average over a special measure called the repeller measure: $t_f|_{q=1} = 1/\Lambda_f$. Seeing the escort averaged $\ln \Lambda$ and $\ln \lambda$ as characteristic exponents, Eq. (10) takes the form of the Liapunov dimension D_L in two dimensions, showing that the Kaplan-Yorke conjecture $D_L = D_1$ holds in a generalized form for two-dimensional hyperbolic systems.

For chosen values of the pruning parameters i_0 and i_1 , all fundamental orbits are first identified and then the smallest root of the ζ function (6) yields $\tau(q)$. The weights in the escort average (11) are then found and thus $\alpha(q)$ from (10). The spectrum $f(\alpha)$ is found as a parametric plot of $f(q) = q\alpha(q) - \tau(q)$ versus $\alpha(q)$.

In Fig. 2 we show the singularity spectrum thus obtained, with the choice of parameters quoted in the caption. The value for Λ_1 is found from the normalization, i.e., by solving (6) when $q=1$ and $\tau=0$. To interpret this, and to see the role played by particular periodic orbits, it is instructive to associate a pointwise dimension α_f to a single fundamental orbit $0^k 1^l$. From the escort average expression for α , Eq. (10), this is $\alpha_{kl} = 1 - \ln \Lambda_{kl} / \ln \lambda_{kl}$, so

$$\alpha_{kl} = 1 - \frac{x \ln \Lambda_0 + \ln \Lambda_1}{x \ln \lambda_0 + \ln \lambda_1}, \quad (12)$$

where $x = k/l$ is the fraction of zeros to ones in the cycle.

With complete dynamics the asymptotes for Eq. (12) are $1 - \ln \Lambda_0 / \ln \lambda_0$ and $1 - \ln \Lambda_1 / \ln \lambda_1$ as $x \rightarrow \infty$ and $x \rightarrow 0$, respectively. In Fig. 2 we have plotted α_{kl} and $f(\alpha)$ to get a picture

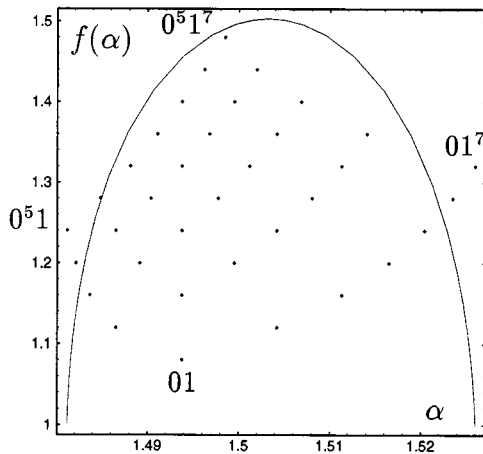


FIG. 2. $f(\alpha)$ spectrum of the pruned Baker’s map $\lambda_0=0.1$, $\lambda_1=0.5$, $\Lambda_0=3$, and $\Lambda_1=1.463\dots$, under the pruning $i_0=5$ and $i_1=7$. Here the points show α_f of the 35 fundamental cycles (x axis) versus a scaled orbit length (y axis). The extreme orbits are labeled by their binary itinerary.

of which orbits predominantly explore which parts of the attractor. In particular $(\alpha_{\max}, \alpha_{\min})$ are given by $(01^{i_1}, 0^{i_0}1)$, explaining why $f(\alpha_{\min})=f(\alpha_{\max})=1$. We will compare this with the result for the Lorenz system in Sec. III.

The escort distribution $\{t_f\}$ can be used in a direct manner to see where an orbit contributes. In Fig. 3 we have plotted $\ln t_f(q)$ for the fundamental cycles of our example system.

We now apply a similar treatment to the spectrum of dynamical scaling indices. The appropriate partition function is

$$\Gamma(q, \gamma) = \lim_{n \rightarrow \infty} \sup_{\sigma \in Z_n} e^{n\gamma} \sum_{i \in \sigma} p_i^q, \quad (13)$$

corresponding to the following choice for a and b in the ζ function (6):

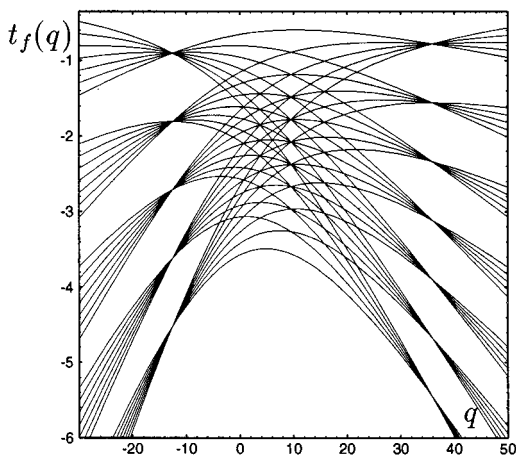


FIG. 3. Logarithm of the escort distribution $\{t_f\}$ versus q , showing the relative importance of fundamental cycles as q is varied. Note the well-arranged transition from five bands of seven weights into seven bands of five weights.

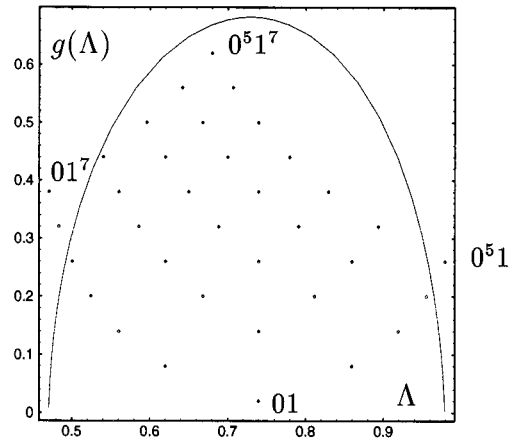


FIG. 4. Spectrum of scaling indices $g(\Lambda)$, and the local Liapunov exponent associated with each of the fundamental cycles Λ_{kl} , again plotted against orbit length.

$$a = \Lambda_0^{-q} e^{\gamma(q)}, \quad b = \Lambda_1^{-q} e^{\gamma(q)}. \quad (14)$$

The leading zero of the ζ function fixes $\gamma(q)$ as for $\tau(q)$ in the $f(\alpha)$ formalism and the generalized exponent is obtained from $\Lambda(q) = d\gamma/dq$. The spectrum of scaling indices then follows from a Legendre transform: $g(\Lambda) = q\Lambda - \gamma(q)$. The $g(\Lambda)$ spectrum of our example system is shown in Fig. 4.

It is instructive to express the local Liapunov exponent $\Lambda(q)$ in the escort average formulation. A variation of $1/\zeta=0$, with respect to q and γ , yields

$$\Lambda(q) = \frac{\langle \ln \Lambda \rangle}{\langle n \rangle}, \quad (15)$$

where n is the length of the symbolic string of the periodic orbits. The escort average now takes the form $\langle Q \rangle = \sum_{\text{FC}} \Lambda_f^{-q} e^{n_f \gamma} Q_f$. Following the earlier discussion concerning α_{kl} , we now consider the local Liapunov exponent of a solitary fundamental cycle Λ_{kl} , finding

$$\Lambda_{kl} = \frac{x \ln \Lambda_0 + \ln \Lambda_1}{1+x}, \quad (16)$$

with $x = k/l$ as the ratio of zeros to ones as before. In Fig. 4, Λ_{kl} for the fundamental cycles is plotted against their (rescaled) length $k+l$. Note the reversal of which orbits contribute to which part of the spectrum from the case of $f(\alpha)$ in Fig. 2.

The above results are all based on an exact block pruning rule. This is only true for special choices of ϵ_0 and ϵ_1 in Fig. 1. We will here examine what happens at other values. As ϵ_0 and ϵ_1 vary, periodic orbits are removed in a well-ordered manner determined by the ordering of their binary value in relation to the kneading sequence [14]. Suppose ϵ_1 is held fixed and ϵ_0 varied. There is a range of values of ϵ_0 , say, $\delta\epsilon_0$, over which orbits with i_0 successive zeros are removed. The kneading sequence determines that, as ϵ_0 increases to $\bar{\epsilon}_0$ say, $0^{i_0}1$ is the first to be removed, $0^{i_0+1}1$ the last to be removed.

For any intermediate choice of ϵ_0 , we may not be able to redefine the symbolic dynamics in a manner giving a finite

number of fundamental cycles. We will then, in addition to the fundamental cycles of type $0^k 1^l$, have an additional set contributing in an unshadowed way to $1/\zeta$. However, these orbits necessarily contribute values for α in the range $(\alpha_{\min}, \alpha_{\max})$ and the weights associated with such orbits will be small.

It is our contention that these contributions to the ζ function will not alter $f(\alpha)$ significantly [nor $g(\Lambda)$]. We defer further discussion of this point until Sec. III, where the same situation arises in the topology of the Lorenz system, but with more interesting results.

C. Correspondence with Bernoulli trials

We conclude this section with a somewhat quirky application of the ζ formalism—more to demonstrate the scope of the technique than anything else—where we associate the dynamics of the map (4) with a sequence of Bernoulli trials where 0 denotes “success” and 1 denotes “failure” and assume that these two possible outcomes occur with probabilities p and $q=1-p$, respectively. For simplicity we let the pruning be symmetric: $i_0=i_1=i$.

We are interested in the probability of doing n trials, without i successive successes or i successive failures, given that the series contains m failures. Knowing this probability, say $u_m(p)$, we can rewrite the partition function (7) as a sum over the number of zeros in the string:

$$\begin{aligned}\Gamma(q, \tau) &= \lim_{n \rightarrow \infty} \sum_{m \in [0, n]} \binom{n}{m} u_m(p) a^m b^{n-m} \\ &= \lim_{n \rightarrow \infty} b^n \Omega(a/b),\end{aligned}\quad (17)$$

where the last expression follows on introducing the generating function

$$\Omega(s) = \sum_{m \in [0, n]} \binom{n}{m} u_m(p) s^m. \quad (18)$$

Using standard techniques of probability theory [15], we can find the probability of not seeing i successive zeroes or ones as

$$w_n(p) = \eta(x_p) \left(\frac{1}{x_p} \right)^n, \quad (19)$$

where x_p is the smallest positive root of

$$x - x^i(pq^{i-1} + qp^{i-1}) + (pqx^2)^{i-1} = 1. \quad (20)$$

The function $\eta(x)$ does not depend on n and is bounded in x .

The probability we require to simplify the partition function $u_m(p)$ is a conditional version of $w_n(p)$, so the relation between the two is

$$w_n(p) = \sum_{m \in [0, n]} \binom{n}{m} u_m p^m q^{n-m} = q^n \Omega(p/q). \quad (21)$$

We now use p as a free parameter in $[0, 1]$, and by choosing $p = a/(a+b)$, we can combine (19) and (21) to eliminate $\Omega(a/b)$ from (17) and find

$$\Gamma(q, \tau) = \lim_{n \rightarrow \infty} \left(\frac{a+b}{x_p} \right)^n \eta(x_p). \quad (22)$$

Requiring that $\Gamma(q, \tau)$ is finite and nonzero, we find $x_p = a+b$, which upon insertion in (20) yields

$$a+b - ab(a^i + b^i - a^i b^i) = 1.$$

This is also what $1/\zeta=0$ and Eq. (6) give, for the case $i_0=i_1=i$.

In this way we see that, for this system, we could have used the theory of recurrent events from probability theory to do the resummations otherwise done by the cycle expansions of $1/\zeta$. It also illustrates the wide scope of the ζ -function formalism.

III. THE MULTIFRACTALITY OF LORENZ

Consider now the Lorenz equations (3) at the parameter values $(r, \sigma, b) = (28, 10, 8/3)$. Orbits quickly contract onto a butterfly-shaped object with complex metric and statistical properties, which we here will describe using the multifractal formalism. We observe the attractor using a Poincaré section at $z=r-1$ and contained within the region bounded by the two fixed points in this plane. This yields two branches where the unstable manifold of the two symmetric fixed points cross the section. Assuming the measure to be smooth along the orbits (Sinai, Ruelle, and Bowen), we set out to describe the multifractal properties of the dynamics along the branches.

The classical method used in [1] to find $f(\alpha)$ involves finding the unique $\tau(q)$ that holds the partition function (7) finite as the partition becomes infinitely fine and then use the Legendre transform to obtain $f(\alpha)$ as discussed previously. Here we use the direct approach (10), based on the escort average, with the weights $t_p = \Lambda_p^{-q} \lambda_p^{q-\tau-1}$, where $\Lambda_p > 1 > \lambda_p$ are the Floquet multipliers, that is, the eigenvalues of the Jacobian matrix of orbit p .

A. A hierarchy of partitions

The simplest symbolic description we can give the system is to record which branch an orbit visits, i.e., a zero if the orbit visits the left branch ($x < y$) and a one otherwise. At our choice of parameters, this yields a generating partition: Any point is uniquely represented by the symbolic itinerary of the trajectory starting at this point. A finite itinerary, on the other hand, defines a segment.

We construct a hierarchy of Markov partitions in the following way. Let a segment of a partition on the n th level be the collection of points with the same n first symbols in their itinerary. These points constitute connected regions, and as we increase n , we create successively finer partitions, as illustrated in Fig. 5. The segments are ordered along the branches after the binary value of their labels, showing a twisted horseshoe topology.

B. Finding the periodic orbits

The Lorenz system is symmetric under S : $(x, y, z, t) \rightarrow (-x, -y, z, t)$, which in symbol space corresponds to an interchange of 0 and 1. So orbits symmetric under S have the same eigenvalues, a fact that at string

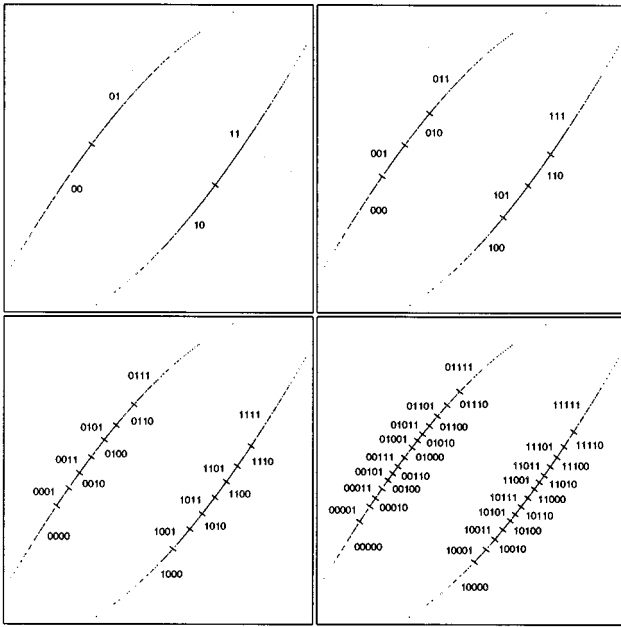


FIG. 5. Levels 2–5 in the hierarchy of partitions generated by the binary dynamics.

length 16 reduces the number of cycles we need to find from 8798 to 4418. We are at present able to find all orbits of symbolic length 16 or less in the following way. First, search a long (10^6) symbolic itinerary for the substring most compatible with repetitions of the cycle itself, its S -symmetric orbit, or any permutation of the two. The point corresponding to the first symbol of this substring is then read from a disk and used in a Newton-Raphson method [14] to localize the orbit to within the accuracy of the numerical integration, 10^{-10} .

The Jacobian matrix is then found [14] by integrating six partial derivatives of the coordinates with respect to the initial condition along the found orbit. The largest eigenvalue of this matrix is Λ_p . As $\Lambda_p/\lambda_p \gg 1$ and λ_p becomes very small, λ_p is best found using the dissipation $\Lambda_p \lambda_p = e^{-\delta T_p}$, where $\delta = \sigma + b + 1 = 41/3$ and T_p is the orbit period. Since $1/\zeta$ is very sensitive to small changes in τ when $|q|$ is large, $\tau(q)$ is found through bisection rather than a Newton search. Instead of differentiating $\tau(q)$ numerically, we now use the escort average (10) to determine $\alpha(q)$ and then find the spectrum through $f(\alpha) = q\alpha - \tau(q)$.

We used an Adams-Bashforth five-step method as predictor, corrected by an Adams-Moulton four-step method, giving a total error of order h^4 , where h is the step size. All calculations were done using quad precision and $h^4 = 10^{-10}$.

At the chosen parameter values, pruned orbits are experimentally found [14] to contain the substrings 0^{25} or 1^{25} , at least as a first approximation. We first assume this empirical observation to be exact and will return to what happens if this is not the case in Sec. IV. The pruning rule is then of the block form as in the case of the pruned Baker's map in Sec. II, with fundamental cycles of the form $\text{FC} = \{0^k 1^l\}_{k,l \in [1,i]}$. The Lorenz dynamics thus corresponds to a symmetric multinary dynamics of order $24^2 = 576$ and we can find an efficient expansion of $1/\zeta$.

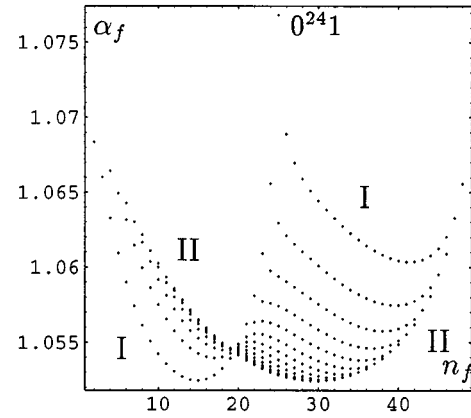


FIG. 6. Pointwise dimension of the fundamental cycles $\alpha_f = 1 - \ln \Lambda_f / \ln \lambda_f$ versus n_f . Orbits along branch I have the form $0^k 1$, while those along II have the form $0^{n_f/2} 1^{n_f/2}$ if n_f is even; otherwise $0^{(n_f+1)/2} 1^{(n_f-1)/2}$.

To find the fundamental cycles, we need a better method than the one above, as the cycles now range from 2 to 48 in length. As seen in Fig. 5, the symbolic dynamics poses a strict ordering of the symbol sequences along a branch. This can be used directly in a bisective hunt along linearized sections of the branch to find any periodic orbit of length less than ~ 50 . Implementing this [11], we are able to find all fundamental cycles within the accuracy of the integration. In Fig. 6 we show the values for α_{kl} for different fundamental orbits, determined from $\alpha_{kl} = 1 - \ln \Lambda_{kl} / \ln \lambda_{kl}$, against the orbit length n_f .

C. Cycle expansion of the Lorenz system

The redefinition of the alphabet makes the expansion of $1/\zeta$ more efficient. The first two curvature corrections are

$$c_5 = 2t_{00101} - 2t_{001t_{01}},$$

$$c_6 = 2t_{000101} + 2t_{001011} - 2t_{01t_{0001}} - t_{01t_{0011}} - t_{001t_{001}},$$

which can be seen to vanish if $t_p = 1$ or if $t_p = a^{n_0} b^{n_1}$. We have successively included the effects of the curvature corrections up to orbit length 16 in Eq. (5) and derived the corresponding singularity spectra: These are found to differ by at most 10^{-4} ; see Fig. 7. In Fig. 8 we show the spectrum of singularities for the Lorenz equations, calculated using all fundamental cycles and curvature corrections up to and including c_{16} .

The previous results are combined in Fig. 9 to show both $f(\alpha)$ and α_{kl} , the pointwise dimension of the fundamental cycles. For α_{kl} , the abscissa is proportional to $n_f = k + l$, the symbolic length of the orbit, as before. The purpose of this figure is to show where in the α domain a certain cycle contributes. Figure 9 can be compared with Fig. 2, from the pruned Baker's map. A more complex structure is immediately apparent: The cycle distribution is skew symmetric, with relatively few cycles contributing to larger values of α . These features are generally explained by the fact that there is a range of values for the expanding eigenvalue Λ_f , for orbits of fixed length n_f , as shown in Fig. 10. Another

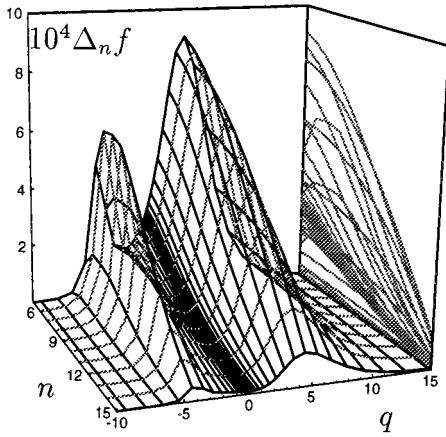


FIG. 7. Convergence of $f(q)$ as the curvature corrections are included. Plotted is (up) $10^4 \times [f_n(q_i) - f_{16}(q_i)]$ versus (forward) n , the longest curvature correction included, and (across) q_i . For each n a new $\tau(q)$ is found.

new feature also emerges: cycles can now become homoclinic at appropriate values of the parameter r . We will return to the effects of this later.

To complement the above, we show also the spectrum of scaling indices $g(\Lambda)$, obtained as explained in Sec. II, using Eq. (5) for the dynamical ζ function, now with the cycle weight $t_p = \Lambda_p^{-q} \lambda_p^{n_f \gamma}$. Results are shown in Fig. 11. In this case we have ignored the curvature corrections, i.e., set $c_n = 0$ for all n .

IV. DISCUSSION

In applying the cycle expansions of Eq. (5) to the Lorenz case we have assumed that the topology is such that we can find the set of fundamental cycles. In the case of a block

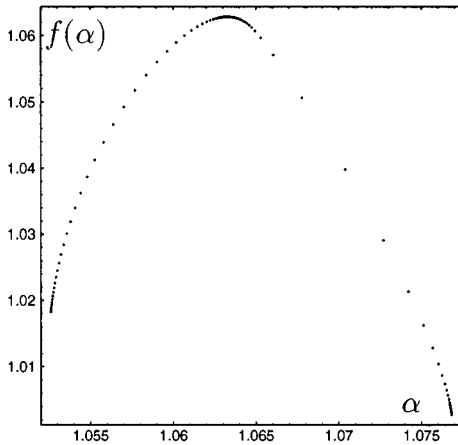


FIG. 8. Spectrum of singularities $f(\alpha)$ for the dynamics in the Poincaré section of the Lorenz system, found using the 300 fundamental cycles corrected with the 10 135 elements from the PPC \setminus FC (that is, elements from the power set of prime cycles excluding the fundamental cycles) of total length less 16 or less. [By assuming the measure to be smooth along the orbits, $f_{\text{Lor}}(\alpha) = f(\alpha) + 1$.]

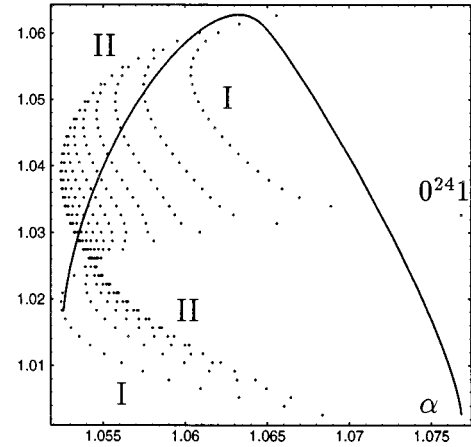


FIG. 9. Combination of $f(\alpha)$ and α_f , the pointwise dimension of the fundamental cycles. For the fundamental cycles, the y value is proportional to the length of the orbit. The purpose is to show where in the α spectrum a certain cycle contributes. The labels I and II are as in Fig. 6.

pruning rule as above, this is possible, but as we vary r , the pruning rule also changes. We here examine how this affects the cycle expansions.

At the parameter values of interest, homoclinic orbits exist for a dense set of r values. As r is increased from its critical value $r_0 \cong 24.67$, orbits become homoclinic in a well-defined manner [14]. All periodic orbits with more than 26 identical successive zeros or ones are removed in homoclinic explosions as r is increased to a value $r \cong 26.63$. The manner in which the family of prime cycles of the form $0^{26}1s$, where s is an admissible sequence, is removed is the same as for the previous families $0^{27}1s$, $0^{28}1s$, etc.: The prime cycle $0^{26}1$ is the first of this family to become homoclinic, at $r_{\text{min}} \cong 26.3$. The other members of this family follow, with increasing binary value of their label, until, at $r_{\text{max}} \cong 26.7$, the orbit $0^{26}1^{26}$ acquires homoclinic status. The next family to go, $0^{25}1s$, behaves in a different manner, as shown in Fig. 12. When $r \cong r_{\text{max}}$ the first member of this family acquires homoclinic status as for the other families and, as r is increased, orbits with higher binary labels are pruned. Now,

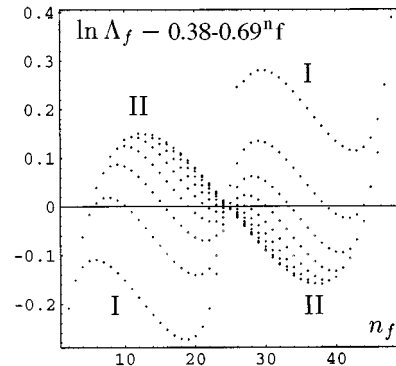


FIG. 10. Logarithm of the expanding eigenvalues of the fundamental cycles. Plotted is the difference from the exponential fit: $\ln \Lambda_f - 0.38 - 0.69^{n_f}$ versus n_f . The labels I and II are as in Fig. 6.

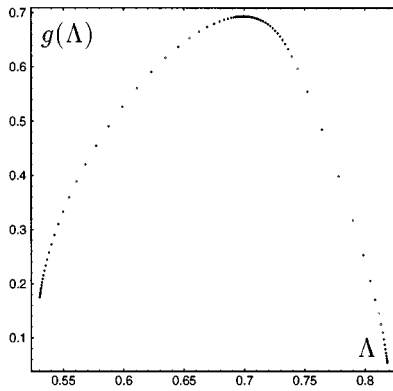


FIG. 11. Spectrum of scaling indices $g(\Lambda)$ of the Lorenz equations. This curve was found using only the 300 fundamental cycles, assuming that all curvature corrections are negligible.

however, this trend turns, for $r \cong 27.5$, and the pruned orbits again become admissible. In Fig. 12 we show how α_f depends on r for some orbits at the extreme part of the spectrum. Note the periodic orbit $0^{25}1^3$, which is not pruned in this region of r , showing that the block pruning rule is only approximative. Including this orbit at $r=28$ will move α_{\max} to about 1.082. This illustrates the sensitivity of the right-hand part of $f(\alpha)$ to the effect of a small correction of the pruning rule.

Denote the fundamental cycles of the form 0^{k1^l} the ‘‘block’’ fundamental cycles. Of these, we see that 0^{241} is the one closest to becoming homoclinic. Following the orbit as we change r , however, we see (Fig. 12) that this never happens, consistent with the observation in [14] that i decreases to 24 as r approaches 28, but then increases.

For the homoclinic case, one can estimate the pointwise dimension α_{\max} using the linearized flow around the origin and the Kaplan-Yorke conjecture that the pointwise dimension equals the Liapunov dimension, giving

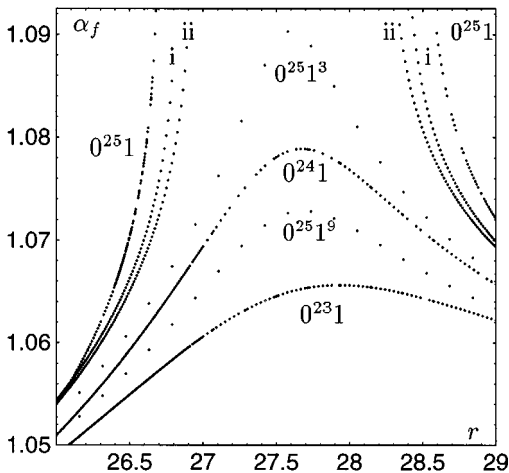


FIG. 12. Following some extreme orbits as r is varied. Plotted is the pointwise dimension α_f versus r . The orbits marked i and ii are $0^{25}1001$ and $0^{25}101$.

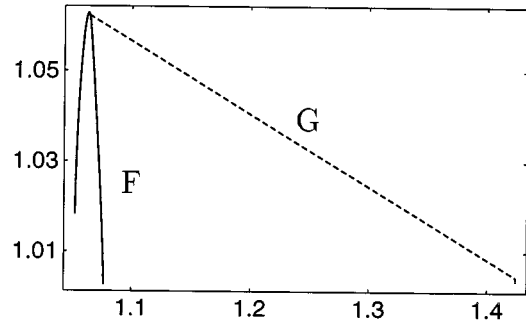


FIG. 13. Conjectured effect of the set G of fundamental cycles on $f(\alpha)$ (dashed line) together with $f(\alpha)$ from the block fundamentals F (solid curve).

$$\tilde{\alpha}_h = \alpha_h + 1 = 3 + \frac{\delta}{\nu_3}, \tag{23}$$

where ν_3 is the smallest of the linearized eigenvalues of the origin, i.e., $\nu_3 = -(\sigma + 1)/2 - [\sqrt{(\sigma - 1)^2 + 4\sigma r}]/2$, and $\delta = \sigma + b + 1 = 41/3$. This gives $\alpha_h \cong 1.4$ in this region of r .

At any value of r in the range of interest there are periodic orbits close to the homoclinic orbit and these may be fundamental cycles, though not of the block type, for example, $0^{25}101$, which, for lower r values, contributes to $1/\zeta$ through the correction term

$$c_{0^{25}101} = t_{0^{25}101} - t_{0^{25}1}t_{01},$$

but becomes a fundamental cycle as $0^{25}1$ becomes homoclinic. The expansion of the ζ function is therefore amended to read

$$\frac{1}{\zeta} = 1 - \sum_{f \in F} t_f - \sum_{g \in G} t_g - \sum_{c \in C} t_c, \tag{24}$$

where F is the block fundamental cycles, G is the set of fundamental cycles not in F , and C is the set of elements from PPC making up the curvature corrections. The sets C and G thus vary with r , taking into account how the pruning rule changes.

We conclude with the following *conjecture*: The main effect of the fundamental set G is to alter the $f(\alpha)$ curve from that shown in Fig. 8(a) to the curve in Fig. 13. Here the downward sloping part has been connected to the point α_h , corresponding to the homoclinic orbit. The following observations support this conjecture.

The Lorenz system is nonhyperbolic; in particular it supports homoclinic orbits, which, in the parameter range of interest, are dense in r . A (near-)homoclinic orbit connects two quite distinct regions of the attractor: the butterfly-shaped object, where a typical orbit spends most of its time, and the seldom visited origin. The role of the homoclinic is to induce a phase transition [17] at some appropriate negative value of q , manifest as a flat part of the $f(\alpha)$ curve [recall that $q = f'(\alpha)$]. Such phase transitions are common in other nonhyperbolic systems [16,17], where they again distinguish between different parts of the attractor. One difference in the system considered here is the linking of these

transitions with homoclinic orbits. In a recent study of the logistic map (a nonhyperbolic system) [17], it was argued that for $q < q_T$, $q_T > 0$ being the critical value where the transition occurs, spectra can be computed using techniques devised for hyperbolic systems. We believe the same argument can be applied here, making allowance for the obvious difference that the origin in the logistic map is a point of maximal measure, whereas here, it is minimal, so the inequality is inverted.

Other members of the set G are long periodic orbits with small values of t_p , having negligible effect in $q > q_T$, but

modifying the curve in $q < q_T$, as shown in Fig. 13. This point is under further study.

ACKNOWLEDGMENTS

We thank C. Sparrow for useful discussions. K.O.W. would like to thank the Norwegian Research Council for financial support under Project No. 100231/410, and also acknowledges support from the Cambridge Philosophical Society.

-
- [1] T.C. Halsey, M.H. Jensen, L.P. Kadanoff, I. Procaccia, and B.I. Shraiman, *Phys. Rev. A* **33**, 1141 (1986).
 - [2] H.G.E. Hentschel and I. Procaccia, *Physica D* **8**, 435 (1983).
 - [3] J.-P. Eckmann and I. Procaccia, *Phys. Rev. A* **34**, 659 (1986).
 - [4] A. Rényi, *Probability Theory* (North-Holland, Amsterdam, 1970).
 - [5] R. Artuso, E. Aurell, and P. Cvitanović, *Nonlinearity* **3**, 325 (1990).
 - [6] V. Franceschini, C. Giberti, and Z. Zheng, *Nonlinearity* **6**, 251 (1993).
 - [7] B. Eckhardt and G. Ott, *Z. Phys. B* **93**, 259 (1994).
 - [8] E.N. Lorenz, *J. Atmos. Sci.* **20**, 130 (1963).
 - [9] C. Beck and F. Schlögl, *Thermodynamics of Chaotic Systems, An Introduction* (Cambridge University Press, Cambridge, 1993).
 - [10] M. Denker, C. Grillenberger, and K. Sigmund, in *Ergodic Theory on Compact Spaces*, edited by A. Dold and B. Eckmann, *Lecture Notes in Mathematics* Vol. 527 (Springer-Verlag, Berlin, 1976).
 - [11] K.O. Wiklund, Ph.D. thesis, Imperial College, University of London, 1996 (unpublished).
 - [12] A. Cohen and I. Procaccia, *Phys. Rev. A* **31**, 1872 (1985).
 - [13] C. Grebogi, E. Ott, and J.A. Yorke, *Phys. Rev. A* **37**, 1711 (1988).
 - [14] C. Sparrow, *The Lorenz Equations: Bifurcations, Chaos and Strange Attractors* (Springer-Verlag, New York, 1982).
 - [15] W. Feller, *An Introduction to Probability Theory and Its Applications*, 3rd ed. (Wiley, New York, 1968), Vol. 1.
 - [16] E. Ott, C. Grebogi, and J.A. Yorke, *Phys. Lett. A* **135**, 343 (1989).
 - [17] E. Ott, T. Sauer, and J.A. Yorke, *Phys. Rev. A* **39**, 4212 (1989).